Neuro-Oncology 13(9):983–999, 2011.
doi:10.1093/neuonc/nor072
Advance Access publication July 21, 2011

AR42, a novel histone deacetylase inhibitor, as a potential therapy for vestibular schwannomas and meningiomas

Matthew L. Bush†, Janet Oblinger†, Victoria Brendel, Griffin Santarelli, Jie Huang, Elena M. Akhmametyeva, Sarah S. Burns, Justin Wheeler, Jeremy Davis, Charles W. Yates, Abhik R. Chaudhury, Samuel Kulp, Ching-Shih Chen, Long-Sheng Chang, D. Bradley Welling, and Abraham Jacob

Department of Otolaryngology–Head and Neck Surgery, The Ohio State University, Columbus, OH, USA (M.L.B., J.O., V.B., S.S.B., C.W.Y., L.S.C., D.B.W., A.J.); Center for Childhood Cancer, The Research Institute at Nationwide Children's Hospital, Columbus, OH, USA (J.O., J.H., E.M.A., S.S.B., L.S.C.,); College of Medicine, The University of Toledo, Toledo, OH, USA (G.S.); Department of Pediatrics, The Ohio State University, Columbus, OH, USA (E.M.A., L.S.C.); College of Medicine, The Ohio State University, Columbus, OH, USA (J.W., J.D.,); Department of Pathology, The Ohio State University, Columbus, OH, USA (A.R.C., L.S.C.); College of Pharmacy, The Ohio State University, Columbus, OH, USA (S.K., C.S.C.)

Neurofibromatosis type 2 (NF2) is an autosomal-dominant disease that results in the formation of bilateral vestibular schwannomas (VSs) and multiple meningiomas. Treatment options for NF2-associated tumors are limited, and to date, no medical therapies are FDA approved. The ideal chemotherapeutic agent would inhibit both VS and meningiomas simultaneously. The objectives of this study are (1) to test the efficacy of AR42, a novel histone deacetylase inhibitor, to inhibit VS and meningioma growth and (2) to investigate this drug's mechanisms of action. Primary cultures of human VS and meningioma cells were established. *Nf2*-deficient mouse schwannoma and benign human meningioma Ben-Men-1 cells were also cultured. Cells were treated with AR42, and the drug's effects on proliferation and the cell cycle were analyzed using a methanethiosulfonate assay and flow cytometry, respectively. Human phospho-kinase arrays and Western blots were used to evaluate the effects of AR42 on intracellular signaling. The in vivo efficacy of AR42 was investigated using schwannoma xenografts. Tumor volumes were quantified using high-field, volumetric MRI, and molecular target analysis was performed using immunohistochemistry. AR42 inhibited the growth of primary human VS and *Nf2*-deficient mouse schwannoma cells with a half maximal inhibitory concentration (IC_{50}) of 500 nM and 250–350 nM, respectively. AR42 also inhibited primary meningioma cells and the benign meningioma cell line, Ben-Men-1, with IC_{50} values of 1.5 μM and 1.0 μM, respectively. AR42 treatment induced cell-cycle arrest at G_2 and apoptosis in both VS and meningioma cells. Also, AR42 exposure decreased phosphorylated Akt in schwannoma and meningioma cells. In vivo treatment with AR42 inhibited the growth of schwannoma xenografts, induced apoptosis, and decreased Akt activation. The potent growth inhibitory activity of AR42 in schwannoma and meningioma cells suggests that AR42 should be further evaluated as a potential treatment for NF2-associated tumors.

Keywords: Akt, AR42, cell-cycle arrest, HDAC inhibitors (HDACis), meningiomas, merlin, neurofibromatosis type 2 (NF2), *NF2* gene, vestibular schwannomas (VS).

Received October 5, 2010; accepted April 29, 2011.

†Co-first authorship.

Corresponding Author: Abraham Jacob, MD, Department of Otolaryngology – Head and Neck Surgery, The Ohio State University Eye and Ear Institute, 915 Olentangy River Road, Suite 4000, Columbus, OH, USA, 43212 (abraham.jacob@osumc.edu, after 8/1/2011 ajacob@surgery.arizona.edu).
Current affiliation: Department of Surgery, Division of Otolaryngology, University of Arizona, Tucson, Arizona (A.J.)

Neurofibromatosis type 2 (NF2) is an autosomal-dominant disease caused by mutations in the *NF2* gene.[1,2] Patients with NF2 develop multiple nervous system tumors; however, bilateral vestibular schwannomas (VSs) and multiple meningiomas are most common. VSs develop from Schwann cells of the vestibulocochlear nerve, and meningiomas originate from meningothelial cap cells of the arachnoid.[3] Schwannomas are typically benign tumors, although rare malignant forms have been reported.[4] Meningiomas account for approximately 20% of primary intracranial tumors, and the World Health Organization classifies meningiomas as grade I (benign) (80%), grade II (10–15%), and malignant grade III tumors (1–2%).[3,5–7] While NF2 patients develop both VSs and meningiomas synchronously, these tumors can also occur sporadically in non-NF2 patients. In both scenarios, these tumors occur along the skull base and cause hearing loss, tinnitus, cranial nerve palsies, and balance dysfunction.[8–12] When they are large, NF2-associated tumors can compress the brainstem, resulting in hydrocephalus, blindness, stroke, and even death.[13] Current treatment options for VSs and meningiomas are surgical excision, stereotactic radiation, and observation; however, no medical options exist for afflicted patients. The ideal chemotherapeutic agent would demonstrate efficacy against both tumor types and have minimal side effects.

The NF2 gene encodes a tumor suppressor known as merlin, for *m*oesin, *e*zrin, and *r*adixin-*l*ike prote*in*.[1,2] Loss of merlin leads to increased proliferation of Schwann and leptomeningeal cells.[5,14–16] Investigations into the molecular mechanisms underlying tumorigenesis in NF2-deficient cells have identified several potential drug targets. We and others have reported that the absence of merlin results in activation of the phosphoinositide (PI) 3-kinase/Akt pathway[17,18] and Akt inhibition suppresses schwannoma and meningioma growth.[19,20] Therefore, the preclinical development of inhibitors that suppress the Akt pathway may be an effective treatment strategy for VSs and meningiomas.

Histone deacetylase inhibitors (HDACis) are emerging as a new class of antitumor drugs[21–26] due to their ability to promote differentiation,[27,28] induce cell cycle arrest,[29–31] and cause apoptosis.[32,33] The exact mechanisms by which HDACis induce growth inhibition are dependent on cell type and context.[26] Also, several classes of HDACis exist, and their biologic effects, enzyme specificities, and potencies vary greatly.[34] HDACis can cause epigenetic modifications in gene expression;[35,36] however, they can also exert histone-independent antitumor effects through modulation of cell signaling pathways.[21,27,35,36] HDACis have demonstrated in vitro and in vivo biologic activity to inhibit multiple intracranial tumors through a variety of mechanisms.[37–41] For example, HDACis have been reported to interact with the c-Jun N-terminal kinase (JNK) pathway to induce apoptosis.[41,42] A novel phenylbutyrate-based pan-HDACi, AR42 (previously known as OSU-HDAC42; Arno Therapeutics), has been shown to have potent HDAC-inhibitory activity.[43] This particular drug has shown potent antitumor effects in multiple tumor types, at least in part by inhibition of the PI3K/Akt pathway.[43–49] The objective of the current study is to examine the antitumor effect of AR42 on schwannomas and meningiomas and to determine whether treatment efficacy correlates with Akt pathway suppression.

Materials and Methods

Materials

AR42, licensed by Arno Therapeutics, was formulated as a free base and was supplied by Arno.

Tissue Acquisition and Primary Cell Cultures

The Ohio State University Institutional Review Board approved the protocols for human subjects in the acquisition of fresh VS and meningioma specimens. The diagnoses of these tumors were confirmed by a clinical neuropathologist. The excised tumor specimens were placed in Dulbecco's modified Eagle's medium (DMEM) (Invitrogen) with 10% fetal bovine serum (FBS) and promptly transported to the laboratory. Specimens were then minced into 1–3 mm sections and dissociated with 0.6 U/mL collagenase (Serva) and 0.125 U/mL dispase (Invitrogen) for 3–5 hours in a 37°C humidified incubator. The dissociated tissue fragments were then triturated, spun down, and plated onto tissue culture-treated dishes (for meningiomas) or onto dishes coated with poly-D-lysine–laminin (PDLL) (for VS) in DMEM/10% FBS.

Immunofluorescent staining was used to confirm the identity of our primary cultures. Cells plated on chamber slides were fixed for 30 min with freshly prepared 2% paraformaldehyde. All antibody dilutions were made in phosphate buffered saline (PBS) with 10 mg/mL bovine serum albumin and 1 mg/mL saponin, and incubations were performed at room temperature. VS cells were probed with S100 (1:1000, #Z0311: Dako USA), and meningioma cells were probed with epithelial membrane antigen (EMA) (1:1000, clone E29 #M0613: Dako USA) (Fig. 1A). After 2 hours, the cells were washed with PBS and incubated for 1 hour with a 1:1000 dilution of either Oregon Green–488 goat anti-rabbit antibody (S100) or Alexa Fluor–488 goat anti-mouse antibody (both from Invitrogen). Cells were then washed with PBS and visualized by epifluorescence.

The purity of the cultures was also confirmed with light microscopy, and photomicrographs were taken to document cell morphology and to confirm the absence of fibroblasts (Fig. 1B). Small clumps of primary tumor tissue were seen at passage #0 (Fig. 1B); however, a monolayer of cells was demonstrated on ensuing passages. To limit fibroblast contamination, only early passage (1∼5) primary

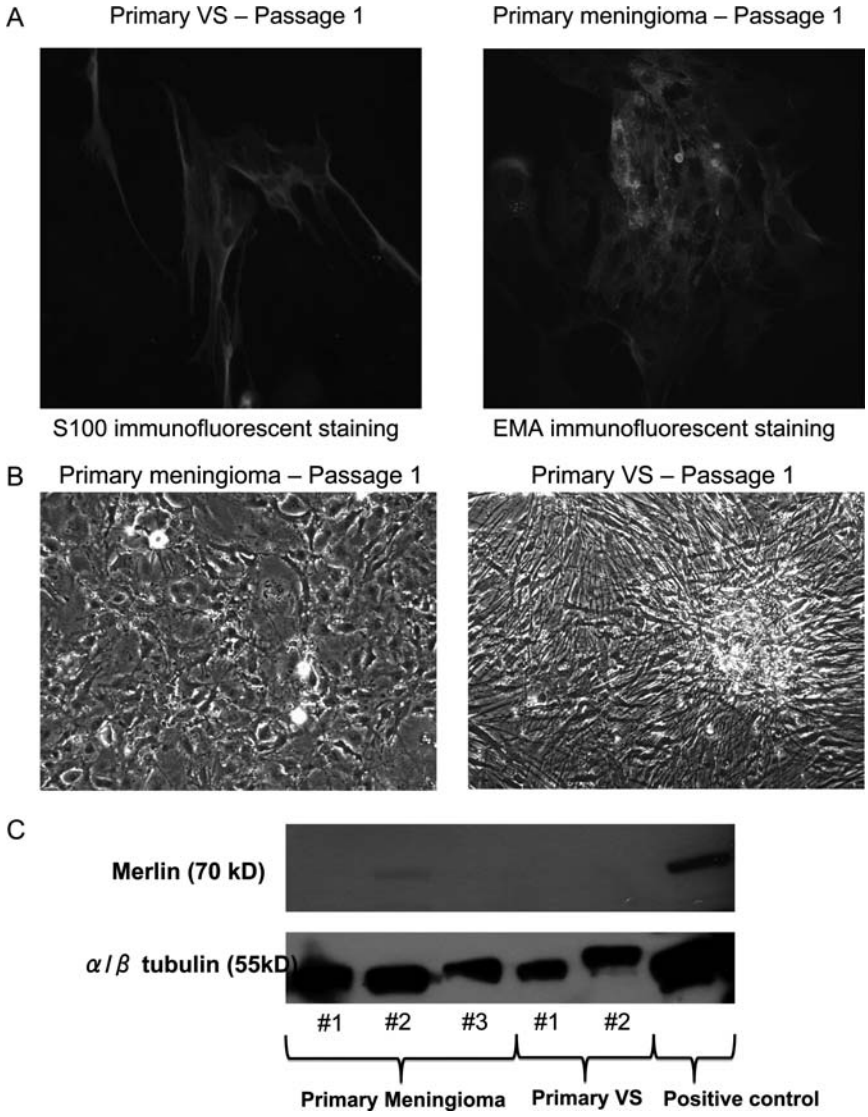

Fig. 1. Identification and characterization of primary VS and meningioma cultures. Immunofluorescence micrographs demonstrating S100 positivity for VS cells and EMA positivity for primary meningioma cells (A). Photomicrographs demonstrating the epithelial-like cell morphology consistent with the original meningioma pathology (Left) and the bland spindle cells with fusiform nuclei characteristic of vestibular schwannoma (Right) (B). Western blotting assessed the merlin status of primary VS and meningioma cells. Only one primary meningioma culture (#2) was weakly positive for merlin, whereas VS and other meningioma cultures were merlin-deficient. The IOMM-Lee (malignant meningioma) cell line was used as a positive control for merlin. Tubulin was used as a loading control (C).

cultures were used for experiments. Prior to each experiment, cultures were examined and fibroblast contamination was less than 10% in each primary culture for each experiment. To determine *NF2* status, Western blots (method below) were performed on untreated primary VS and meningioma cell lysates using an anti-merlin antibody (#3356-1; Epitomics) (Fig. 1C). An antibody to α/β-tubulin (#2148; Cell Signaling Technology) was also used to confirm equal protein loading, and lysate from IOMM-Lee, an $NF2^{+/+}$ malignant meningioma cell line, was used as a positive control. Primary VS and meningioma cells were found to be negative for merlin, with the exception of one primary meningioma culture, which was weakly positive for merlin.

Cell Culture

Both primary human VS and meningioma cells were generated as described above. $Nf2^{-/-}$ mouse schwannoma cells were derived from a *P0Cre;*$Nf2^{flox2/flox2}$ mouse with *Nf2* inactivation in Schwann cells.[19,50] $Nf2^{+/+}$*NF2P2.4-T* schwannoma cells (mSchT) were derived from a transgenic mouse carrying an *NF2* promoter-driven SV40 large T antigen gene.[19,51] Human malignant schwannoma, HMS-97,[52] and Ben-Men-1 benign human meningioma cells[53] were also used. Both $Nf2^{-/-}$ mouse schwannoma and human VS cells were cultured on PDLL-coated dishes and maintained in DMEM/10% FBS containing 10 ng/mL recombinant human NRG1-β1/HRG1-β1

epidermal growth factor domain (heregulin; R&D Systems) and 0.2 μM forskolin (Sigma). All other cell types were plated on uncoated dishes and grown in DMEM/10% FBS.

MTS Assays

Cell proliferation was determined using the CellTiter 96 AQueous Non-Radioactive Cell Proliferation Assay kit (Promega) according to the manufacturer's instructions. Cells were plated at 4×10^3 cells per well in 96-well plates. The following day, cells were treated with AR42 at the indicated concentrations at 37°C. After 72 hours, 20 μL of methanethiosulfonate (MTS) assay solution was added to each well and incubated at 37°C for 1 to 4 hours. The amount of bioreduced formazan produced was estimated by measuring the absorbance at 490 nm. The percentage of cell proliferation was plotted against concentrations of AR42, and the half maximal inhibitory concentration (IC_{50}) was calculated. Cells were also examined by light microscopy to document changes in cell morphology and density.

Westerns and Antibody Arrays

Subconfluent cells were treated with the indicated amounts of AR42. To screen for potential drug-affected signaling pathways, the Human Phospho-Kinase Proteome Profiler antibody array kit was used (R&D Systems), using 300 μg of total protein per array membrane. For immunoblotting, total cell lysates were harvested in ice-cold kinase lysis buffer (20 mM Tris, 150 mM NaCl, 1 mM EDTA, 1 mM ethylene glycol tetraacetic acid, 1% Triton X-100, 2.5 mM sodium pyrophosphate, pH 7.5) supplemented with protease and phosphatase inhibitors (1 mM phenylmethylsulfonyl fluoride, 1 mM sodium orthovanadate, 1x protease inhibitor cocktail [Sigma], and 0.5 mg/mL pepstatin A [Roche]. Lysates were sonicated for 10 seconds, and the total protein content was assayed using the microBCA kit (Pierce). Equal amounts of total cell lysates were resolved by sodium dodecyl sulfate polyacrylamide gel electrophoresis and transferred to PVDF or nitrocellulose membranes. Immunoblots were probed with antibodies against AKT (#9272), phosphoThr308-Akt (C31E5E, #2965), phosphoSer473-Akt (D9E, #4060), stress-activated protein kinase (SAPK)/JNK 56G8 (# 9258), p-SAPK/JNK (Thr183/Tyr185) (#4671), glyceraldehyde-3-phosphate dehydrogenase (14C10, #2118) (all from Cell Signaling Technology), and acetylated histone H3 antibody (#06-599; Millipore).

Cell-Cycle Analysis

Primary tumor and Ben-Men-1 cells treated with the indicated concentrations of AR42 for 2–6 days were harvested by trypsinization. Floating and adherent cells were collected, washed twice with cold PBS then fixed by dropwise addition of 1 mL of ice-cold 70% ethanol while vortexing. A propidium iodide (PI) solution (50 μg/mL) containing RNase A (100 μg/mL) and Triton X-100 (0.05%) was added to the samples, followed by incubation for 30 to 60 min at 37°C. Samples were then filtered to remove cell aggregates and analyzed by FACS (fluorescence-activated cell sorting) Calibur flow cytometer (Becton Dickinson) after gating (FL2-A/FL2-W) the diploid population. Data were analyzed using ModFit LT software (Verity Software House) with gating around the diploid population of cells.

HMS-97 Schwannoma Xenografts, MRI, and Immunohistochemistry

The Ohio State University and Nationwide Children's Hospital Institutional Animal Care and Use Committees approved the animal protocols (2008A0035 and AR07-00062, respectively) for the HMS-97 schwannoma xenograft model, which has been previously described.[19] HMS-97 schwannoma cells (5×10^5 cells/mouse) resuspended in 0.2 mL of a 50% Matrigel solution (BD Biosciences) were injected subcutaneously with an 18-gauge needle into the left flank of severe combined immunodeficiency (SCID) mice (CB-17/Icr SCID from Charles River). On day 3 postinjection, the injected mice were then divided into two groups: the first (control) group of mice was fed normal rodent chow (Harlan Teklad); and the second group of mice was fed chow formulated to deliver 25 mg/kg AR42 daily (Research Diets). Forty-five days after injection the mice were scanned by a high-bore small-animal MRI, using a Bruker Biospin 94/30 magnet (Bruker Biospin). The respiration and temperature of the animals were monitored using the Small Animal Monitoring and Gating system (Model 1025, Small Animals Instruments). Axial T1-weighted (repetition time [TR] = 1500 ms, echo time [TE] = 7.5 ms, Rare Factor = 4, navgs = 4) and T2-weighted rapid acquisition relaxation enhanced (RARE) images (TR = 4200 ms, TE = 12 ms, Rare Factor = 8, navgs = 4) were acquired contiguously over the entire region of the tumor. The acquisition parameters for both the T1- and T2-weighted multislice scans were as follows: FOV = 30 × 30 mm, slice thickness = 1 mm, matrix size = 256 × 256. A region of interest (ROI) that included the tumor was manually outlined (software developed in-house) using the T1- and T2-weighted images. Tumor volumes were calculated from summing the outlined ROI from each contiguous slice.

Following MRI, HMS-97 xenograft tumors in SCID mice with and without AR42 treatment were dissected, fixed in 10% neutral buffered formalin, and embedded in paraffin. Tissue in 5-μm sections were obtained. Standard hematoxylin–eosin staining was performed, as was staining for cleaved caspase-3 (#9661L; Cell Signaling), transferase-mediated dUTP-biotin nick-end labeling (TUNEL) (ApopTag colorimetric assay; Millipore), and phosphoSer473-Akt. Negative controls were treated with the same immunostaining procedure except without the primary antibody.

Results

AR42 Inhibits the Proliferation of Schwannoma and Meningioma Cells

Two mouse schwannoma cell lines (P0Cre;Nf2$^{flox2/flox2}$ and mSchT), a malignant human schwannoma cell line (HMS-97), and a benign meningioma cell line (Ben-Men-1) were used in the initial screen for the efficacy of AR42. Exposure of mouse schwannoma cell lines (P0Cre;Nf2$^{flox2/flox2}$ and mSchT) to AR42 inhibited cell proliferation in a dose-dependent manner ($IC_{50} = 250$ nM) (Fig. 2A). AR42 treatment of primary human VS cells from 3 different patients and HMS-97 human malignant schwannoma cells resulted in similar growth inhibition with a mean IC_{50} of 500 nM and 350 nM, respectively (Fig. 2B). Meningioma cell proliferation was also inhibited by AR42, although these cells were less sensitive than schwannoma cells (Fig. 2C). When primary human meningioma cells from two different patients were treated with AR42, an average IC_{50} of 1.5 μM was obtained. The IC_{50} for the benign meningioma cell line, Ben-Men-1, was found to be about 1 μM. Both VS and meningioma cells treated with AR42 also exhibited a dose-dependent growth inhibition, as observed by light microscopy (Figs 2D and E). These results indicate that AR42 potently inhibits both schwannoma and meningioma cells.

AR42 Decreases Phospho-Akt and Inhibits Histone Deacetylases in NF-associated Tumors

To examine the effects of AR42 on intracellular signaling, we screened the phosphorylation status of multiple cellular kinases in sporadic and NF2 VS cells using the human phospho-kinase antibody array (Fig. 3). Incubation of these membranes with cell lysates indicates which kinases are activated in these tumors as well as whether these same kinases respond to our candidate inhibitors. Activated Akt was strongly expressed in both sporadic and NF2-associated VS cells. Other activated kinases included ERK1/2, Src, Yes, and FAK. Treatment with AR42 of sporadic and NF2 schwannoma cells resulted in a decrease in phosphorylated Akt. Other kinases or phosphoproteins modulated by AR42 treatment included: ERK1/2, CREB, β-catenin, FAK, Src, and Yes. There was no evidence of baseline JNK activation in VS cells or modulation of the JNK pathway by AR42 exposure.

Data obtained from our antibody array studies were confirmed by Western blots. Protein lysates from control and AR42-treated schwannoma and meningioma cells were analyzed using antibodies to phospho-Akt (serine-473 and threonine-308) as well as total Akt protein. Drug treatment consistently decreased phospho-Akt at both ser473 and thr308 in primary VSs, primary meningiomas, and Ben-Men-1 cells (Figs 4A and B), while the total Akt levels remained constant in all samples. Since there have been reports of HDAC inhibitors activating the JNK pathway,[42,54] we next validated that AR42 did not modulate JNK (Fig. 3) using immunoblots. Again, in line with our antibody array data, phosphorylated and total levels of JNK were unaffected by AR42 treatment (Fig. 4C). Then, to verify that AR42 inhibited histone deacetylase, we probed western blots with an antibody to acetylated histone H3. AR42 treatment resulted in a dramatic increase in histone H3 acetylation for all cell types (Fig. 4D).

AR42 Induces G2 Arrest and Apoptosis in Schwannoma and Meningioma Cells

To characterize the effect of AR42 exposure on the cell cycle, flow cytometry was performed using primary VS and meningioma cells that had been exposed to varied AR42 doses and treated for different durations. After 2 days of AR42 exposure, G_2 arrest was induced in primary VS cells, shifting the percentage of cells in G_2 from 16% (control) to 23% (Fig. 5A). After drug treatment, only a slight increase in the hypodiploid sub-G_1 (apoptotic) fraction was observed. Varying the dose while holding duration of treatment constant at 3 days found a similar pattern of G_2 arrest without any increase in apoptotic fraction (Fig. 5B). Treatment duration was then increased to 6 days to identify late treatment effects on the cell cycle. With prolonged AR42 exposure both G2 arrest and a moderate increase in apoptosis was observed (Fig. 5C).

AR42 treatment of Ben-Men-1 cells showed increases in apoptosis along with an increase in the G_2/M fraction (Fig. 5D). Similar results were observed in cells from two different primary meningioma samples (Figs 5E and F). Prolonged AR42 treatment resulted in a large increase in the percentage of meningioma cells in the apoptotic (sub-G_1) fraction (Fig. 5G).

AR42 Inhibits Proliferation of Malignant Schwannoma Xenografts, Induces Apoptosis, and Suppresses Akt Signaling In Vivo

To test the in vivo efficacy of AR42, SCID mice implanted with HMS-97 cells were fed chow containing AR42. After 45 days of treatment, the tumors in AR42-fed mice were approximately 42% smaller in mean volume than those in the control mice (Fig. 6A). The treated mice demonstrated no overt clinical toxicities. The xenograft tumors harvested from AR42-fed mice showed increased numbers of apoptotic bodies on hematoxylin-eosin sections (Fig. 6B). To confirm the presence of apoptosis after AR42 treatment, both cleaved caspase-3 immunohistochemistry and TUNEL staining were performed. Xenograft sections of AR42 had scattered foci with very high cleaved caspase-3 positivity, while cleaved caspase-3 positivity was much less in control tumors (Fig. 6C). TUNEL staining was also stronger in AR42-treated tumors compared with control tumors

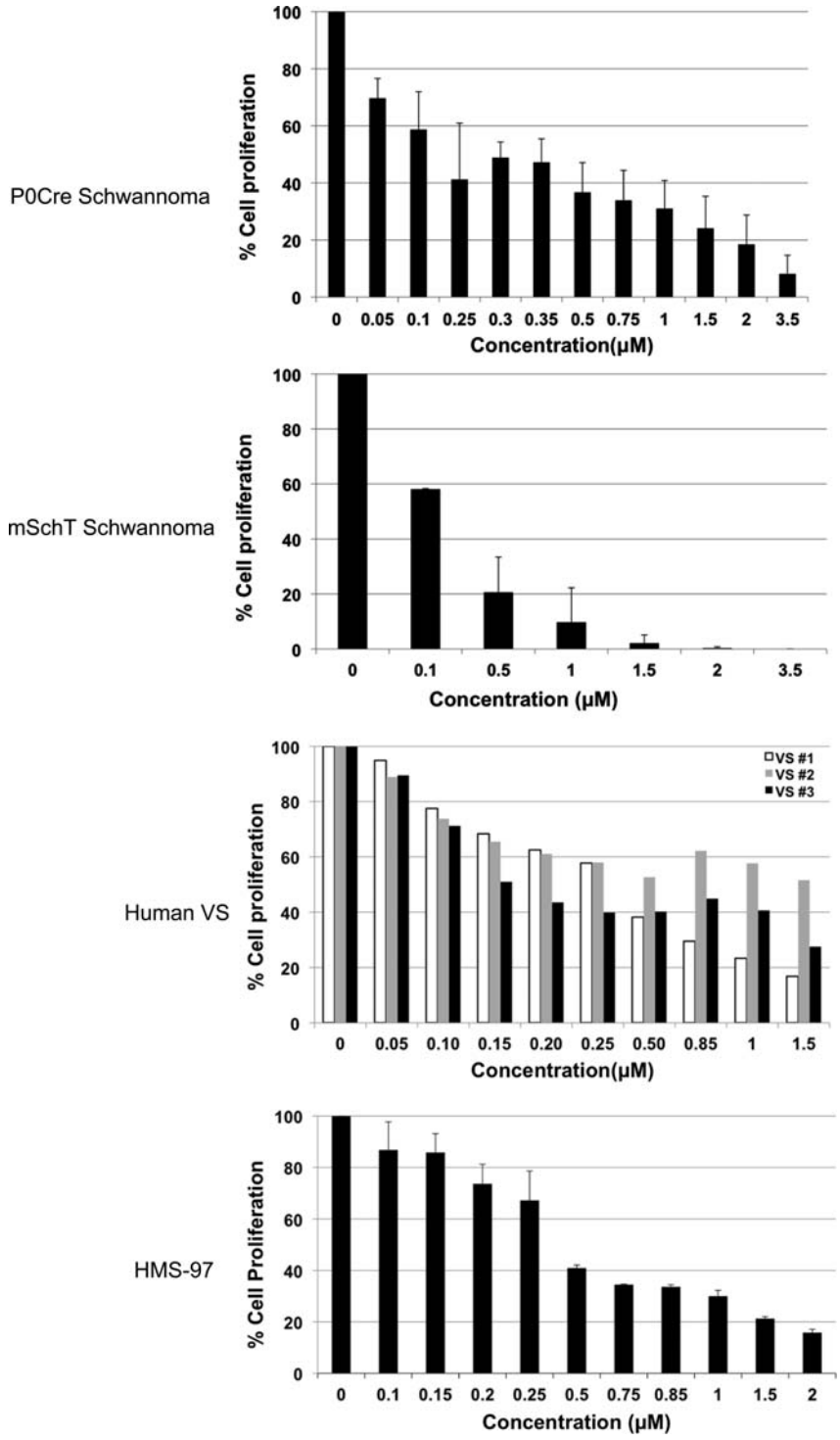

Fig. 2. AR42 potently inhibits the proliferation of schwannoma and meningioma cells. The proliferation of mouse schwannoma cells ($Nf2^{-/-}$ P0Cre;$Nf2^{flox2/flox2}$ and $Nf2^{+/+}$ mSchT) (A), primary human VS and human malignant schwannoma HMS-97 cells (B), and primary human meningioma and the benign meningioma cell line, Ben-Men-1 (C) were inhibited in a dose-dependent fashion following treatment with AR42. Each independent experiment was performed in 4 to 6 replicates. Photomicrographs of primary schwannoma (D) and meningioma (E) cells treated with AR42 revealed significant morphological changes and a dose-dependent decline in cell density.

(Fig. 6D). Akt activation status was then examined in xenograft tumors exposed to AR42 (Fig. 6E). While p-Akt(Ser-473) staining was readily detected in the nucleus and the cytoplasm of untreated xenograft samples, AR42 treatment significantly decreased p-Akt labeling in treated tumors.

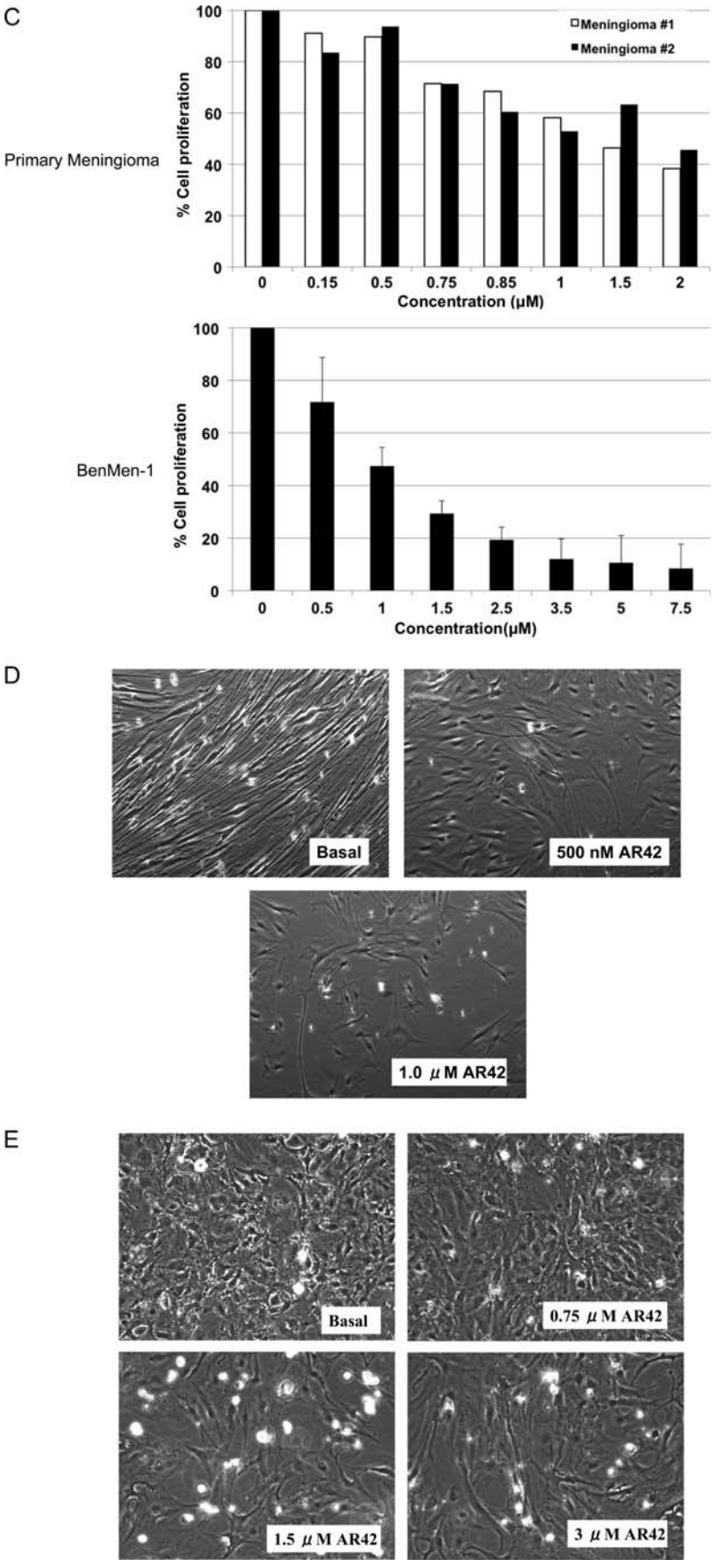

Fig. 2. (continued).

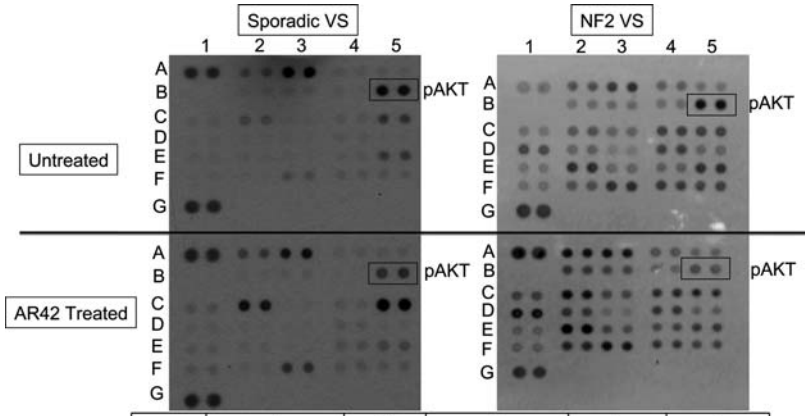

	1	2	3	4	5
A	Positive control	p38 α	ERK1/2	JNK	GSK-3 α / β
B	Blank	MEK1/2	MSK1/2	AMPK α 1	**AKT**
C	TOR	CREB	HSP27	AMPK α 2	B-catenin
D	Src	Lyn	Lck	STAT2	STAT5a
E	Fyn	Yes	Fgr	STAT3	STAT5b
F	Hck	Chk-2	FAK	STAT6	STAT5a/b
G	Positive control	Blank	Negative control	Blank	Blank

Fig. 3. AR42 inhibits Akt phosphorylation in sporadic and NF2-associated schwannoma cells. Primary sporadic and NF2 VS cells were treated with the IC_{50} dose of AR42. The cells were lysed and equal amounts of total protein were incubated with the Human Phospho-Kinase antibody microarray. A decrease in p-Akt(Ser473) was detected in the treated samples. A chart listing the activated kinases represented on the membrane is displayed.

Discussion

Vestibular schwannomas and meningiomas are common, benign intracranial tumors that can cause severe patient morbidity by virtue of their critical locations. For patients with NF2, multiple such tumors occur synchronously and often recur following surgical removal. Currently, no medical therapies are indicated by the U.S. Food and Drug Administration (FDA) for treatment of NF2-associated tumors; therefore, the development of low-toxicity chemotherapeutic agents targeting VSs and meningiomas would be of great benefit. Some NF2 patients are already enrolling in off-label, compassionate-use drug trials for FDA-approved agents.[55–57] For example, inhibitors of vascular endothelial growth factor[58] and ErbB/HER receptors[57] have been used in pilot studies to treat NF2-associated schwannomas; however, response rates have been inconsistent, side effects are significant, long-term benefits are unclear, and these drugs have not been evaluated against meningiomas. Moreover, strong preclinical data supporting use of these drugs for NF2-associated tumors is lacking. The current study demonstrates that AR42, a novel HDACi, potently inhibits both schwannoma and meningioma growth at doses that correlate with Akt inactivation. These same IC_{50} doses cause G_2/M arrest and apoptosis in both cell types. Validation studies in vivo demonstrate that AR42 inhibits schwannoma xenograft growth, induces apoptosis, and decreases activated Akt.

NF2-deficient tumor cells have multiple deregulated signaling pathways, including platelet-derived growth factor, ErbB2/3, PI3K/Akt, MEK/ERK (extracellular signal-regulated kinase), and Rac1/JNK.[59–74] The absence of merlin contributes to Akt activation seen in schwannomas,[32,33,35] and while the signaling pathways involved in meningioma tumorigenesis may be more complex,[75] aberrant Akt activation has been a consistent finding.[18,74] Previous studies demonstrated that Akt inhibition decreases VS cell growth and induces apoptosis both in vitro and in vivo;[19] also, investigators have shown that targeting the PI3–Akt–mTOR (mammalian target of rapamycin) pathway in cultured meningioma cells limits cell growth.[75] Since Akt activation is common to the pathogenesis of both VSs and meningiomas, we assessed whether efficacious doses of AR42 inhibited Akt. Our finding demonstrated that AR42 treatment of both primary schwannoma and meningioma cells consistently resulted in lower levels of Akt phosphorylation, both in vitro and in vivo.

The literature suggests that two plausible mechanisms may account for AR42-mediated decreases in p-Akt. First, AR42 could alter total Akt levels, either by inhibiting transcription/translation of the Akt gene or by destabilizing Akt protein.[46] The second possibility is that AR42 activates an Akt-directed phosphatase that dephosphorylates Akt. Indeed, Chen et al. reported that HDACs 1 and 6 bind to and inhibit protein phospatase-1 (PP1); after HDACi addition, PP1 was liberated from this inhibitory HDAC complex and could dephosphorylate Akt.[43] Since we found no difference in total Akt amounts after AR42 treatment in either schwannomas or meningiomas, we propose that HDAC interaction with Akt may underlie our study's observation that efficacious doses of Akt correlate with decreased p-Akt.

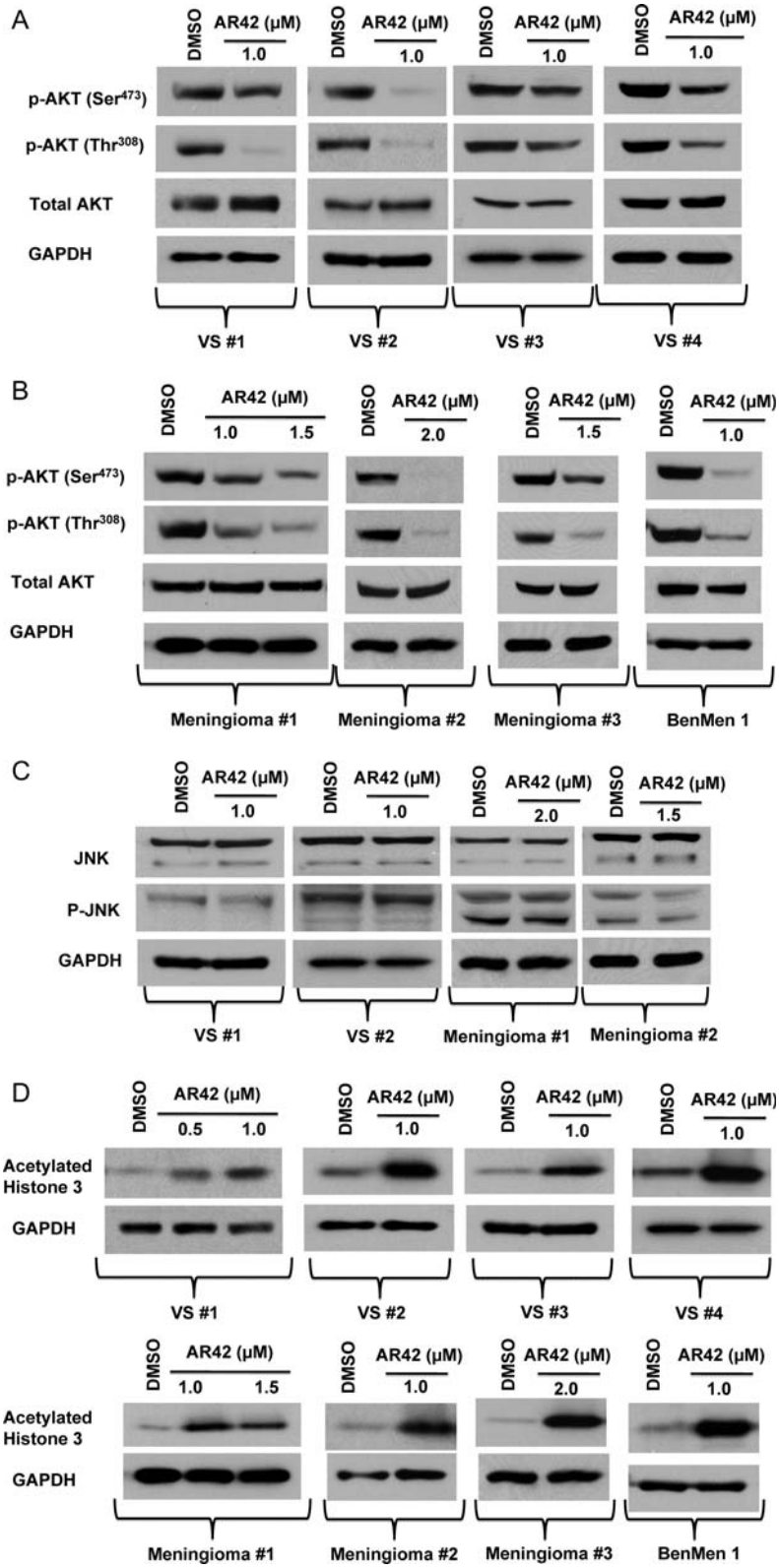

Fig. 4. AR42 decreases phospho-Akt in schwannoma and meningioma cells. Western blots confirmed that AR42 treatment decreased p-Akt levels in primary VS (A) and meningioma cells (B). AR42 treatment did not affect the JNK pathway in meningioma or VS cells (C). The histone deacetylase inhibitory activity as determined by detecting acetylated histone H3 was observed in AR42-treated samples (D).

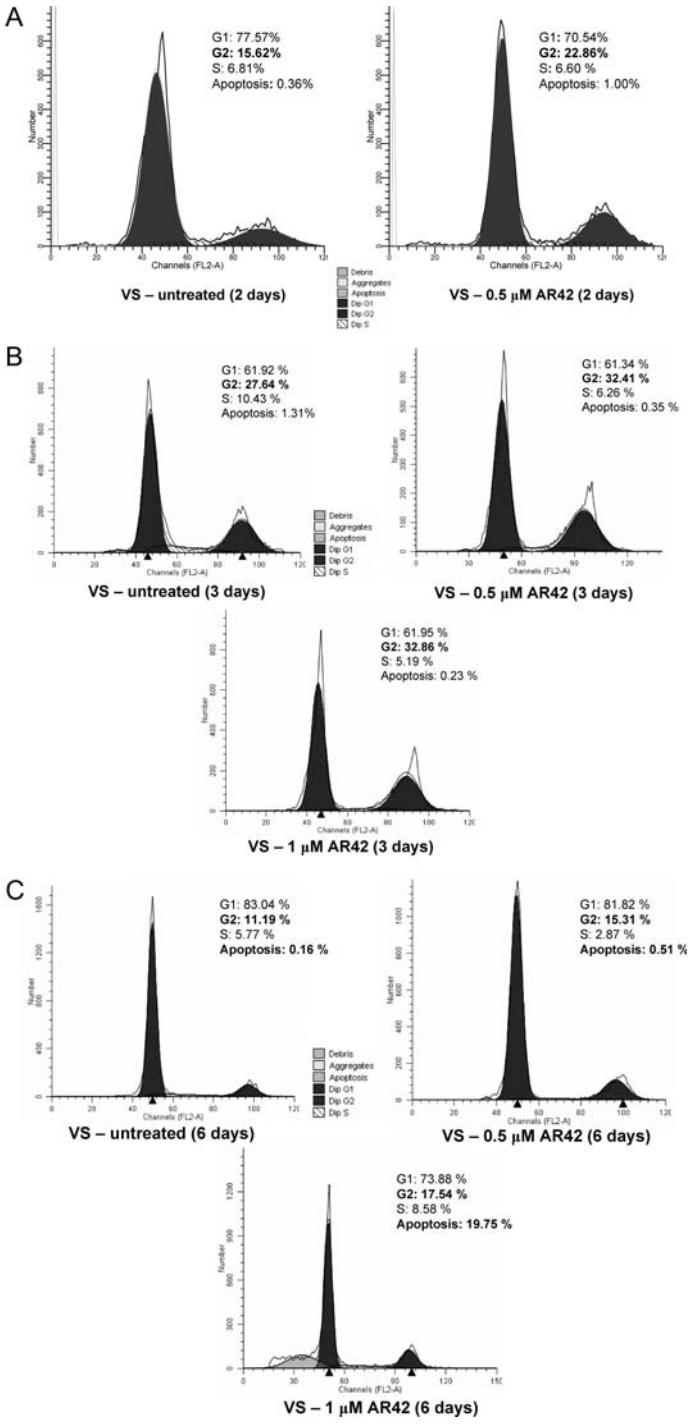

Fig. 5. AR42 affects the cell cycle distribution of VS and meningioma cells. VS and meningioma cells were treated with AR42, as indicated. Floating and adherent cells were collected and fixed in ice-cold 70% ethanol, and the cell cycle distribution was analyzed using propidium iodide labeling. VS treated for 2 days (A) and 3 days (B) with various doses of AR42 demonstrated a dose-dependent G_2 arrest. AR42 treatment for 6 days resulted in G_2 arrest and a moderate increase in apoptosis in VS cells (C). Ben-Men-1 cells (D) were treated with various concentrations and exhibited a dose-dependent increase in G_2 arrest and apoptosis. Primary human meningioma cells from two different patients were treated for 3 days with 0.75 or 1.5 μM AR42 and showed similar increases in the G_2 and sub-G_1 fractions (E and F). After 6 days, AR42-treated meningioma cells showed G_2 arrest and a dramatic increase in apoptosis (G).

Rac1/JNK is deregulated in many glial and Schwann cell tumors, making this a pathway of interest in NF2 research. Kaempfer et al. demonstrated that increases in active Rac1 and JNK play a role in schwannoma progression as well as tumor cell dedifferentiation.[60] By activating apoptotic cascades,[76] JNK sensitizes glioma

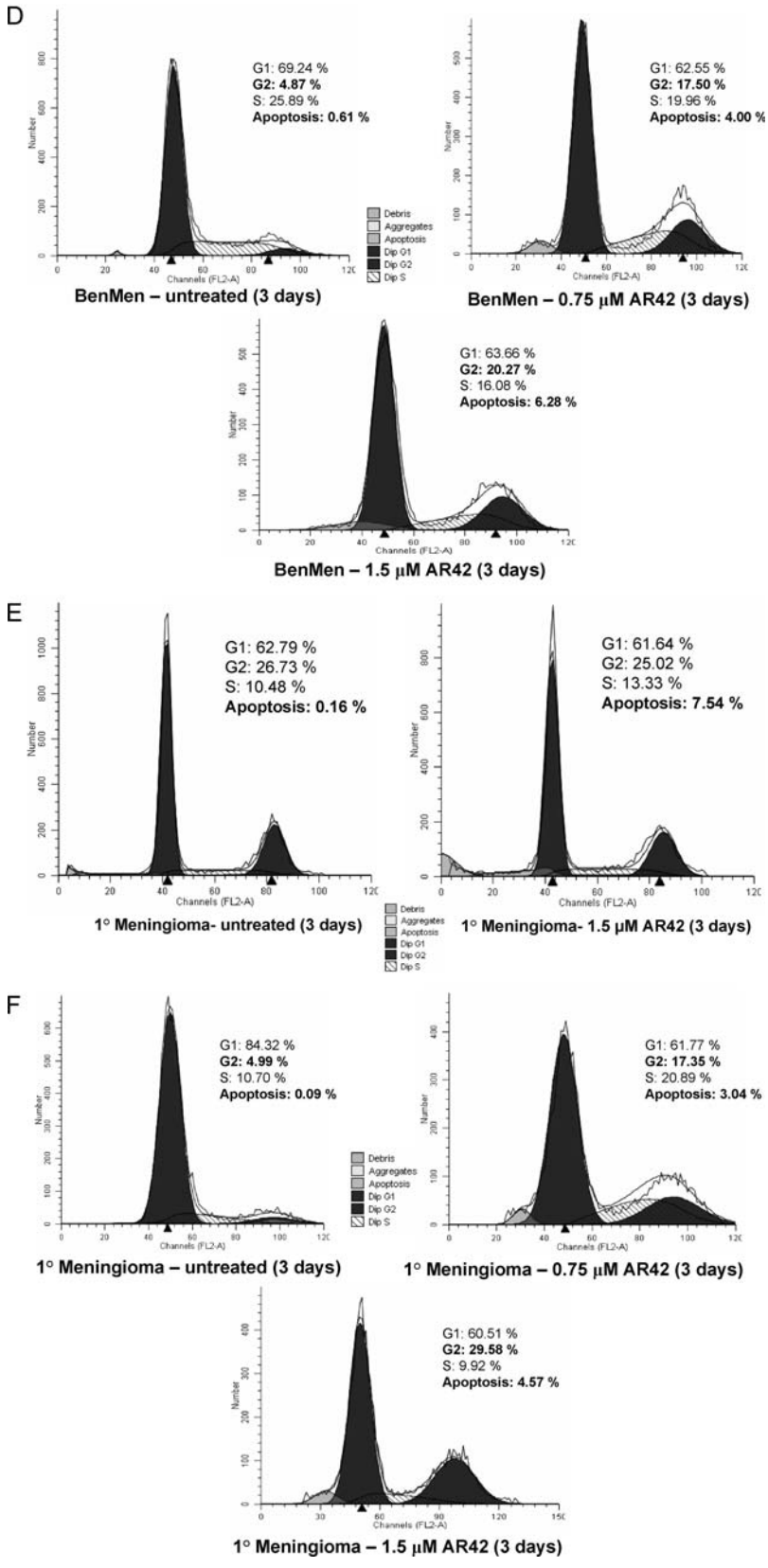

Fig. 5. (continued).

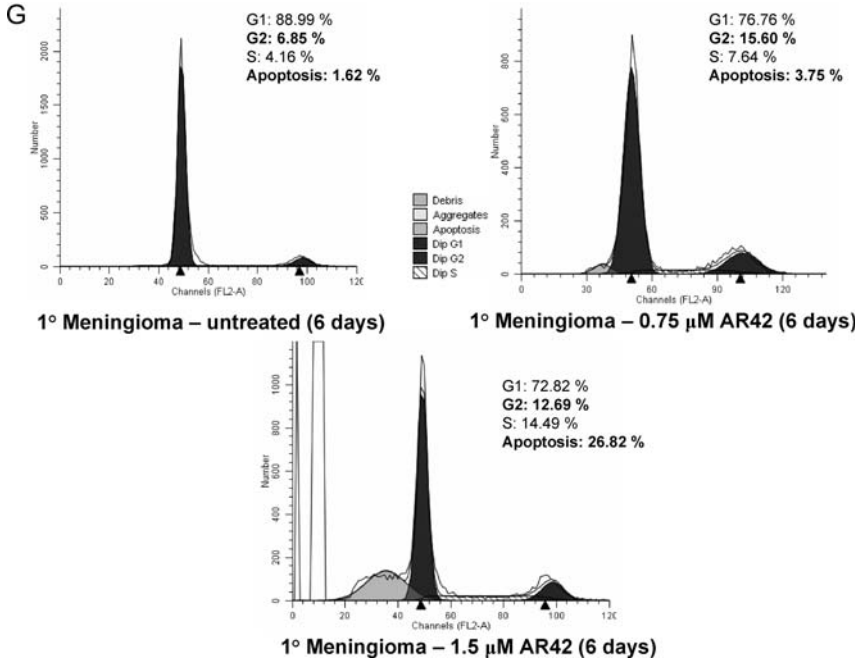

Fig. 5. (continued).

cells to apoptosis.[77] The JNK pathway is a reported target of HDACi in leukemia and glioma cells.[42,78] Ras can also activate JNK,[79] and HDACi treatment can induce apoptosis in cells expressing constitutively active K-RasV12.[54] It is important to note, however, that some HDACi's do not act on the JNK pathway and that this effect may be specific to both HDACi and cell type. For example, Chen et al. demonstrated that the HDAC inhibitors trichostatin A and SAHA (suberoylanilide hydroxamic acid) preferentially promote dephosphorylation of Akt in malignant glioblastoma cells with no effect on the JNK phosphorylation.[43] To examine these pathways in greater detail, we evaluated whether the effects of AR42 may be due to modulation of total JNK or p-JNK levels in NF2-associated tumors. Using phospho-kinase arrays and Western blots, our in vitro results found that AR42 treatment had no effect on total JNK or p-JNK levels, suggesting that JNK signaling does not play a significant role in the antimitogenic effects of AR42 in schwannomas and meningiomas.

Histone acetylation is critical to epigenetic modifications occurring in many solid and hematological tumors.[80,81] Acetylation neutralizes the positive charge on histone tails, thereby weakening interactions with negatively charged DNA, creating a more "open" chromatin conformation and altering transcription of growth-regulatory genes.[35,36] Overexpressed or sustained HDAC activity has been reported in leukemia, lymphomas, and other types of cancers.[21,27,35,36] The aberrant HDAC activity in human neoplasms deacetylates the N-termini of core histones, resulting in a tightly closed chromatin structure; therefore, tumor suppressor genes can be silenced by abnormal HDAC activity. Inhibitors of HDACs reverse this histone deacetylation, thus reactivating expression of silenced genes.[34] Acetylated histones, such H3 and H4, serve as in vitro and in vivo markers for successful HDAC inhibition.[46] We found that AR42 strongly upregulated acetylated histone H3 in treated VS and meningioma cells. Although not the focus of the current study, some of the observed antiproliferative effects of AR42 are likely due to these epigenetic modifications and alterations in gene transcription. These effects are currently under investigation in our laboratory using Affymetrix gene expression arrays and quantitative reverse transcriptase PCR.

HDAC inhibitors profoundly affect cell cycle distribution, potentially inducing arrest at either the G_1 or G_2 checkpoints.[43] Lee et al. reported that the Scriptaid, an HDACi, induced G_1 arrest at low concentrations and G_2 arrest in higher concentrations in colon cancer cells, with no effect on apoptosis.[82] Lin et al. examined the effect of AR42 on a series of malignant mast cell lines and found that AR42 caused G_2 arrest in some cell lines but demonstrated apoptosis in others.[46] We found that AR42 treatment of schwannoma and meningioma cells resulted in dose-dependent G_2 growth arrest in both cell types, consistent with other reports using this inhibitor.[43,46] We also identified apoptosis in both cell types; however, this effect was more pronounced in meningioma cells; VSs demonstrated a moderate increase in apoptosis only after extended treatment (6 days). Consistent with our in vitro data demonstrating that AR42 inhibits schwannoma cell proliferation at doses correlating with decreased p-Akt, our schwannoma xenograft model found that AR42 exposure reduced xenograft tumor volume by 42% (mean), decreased

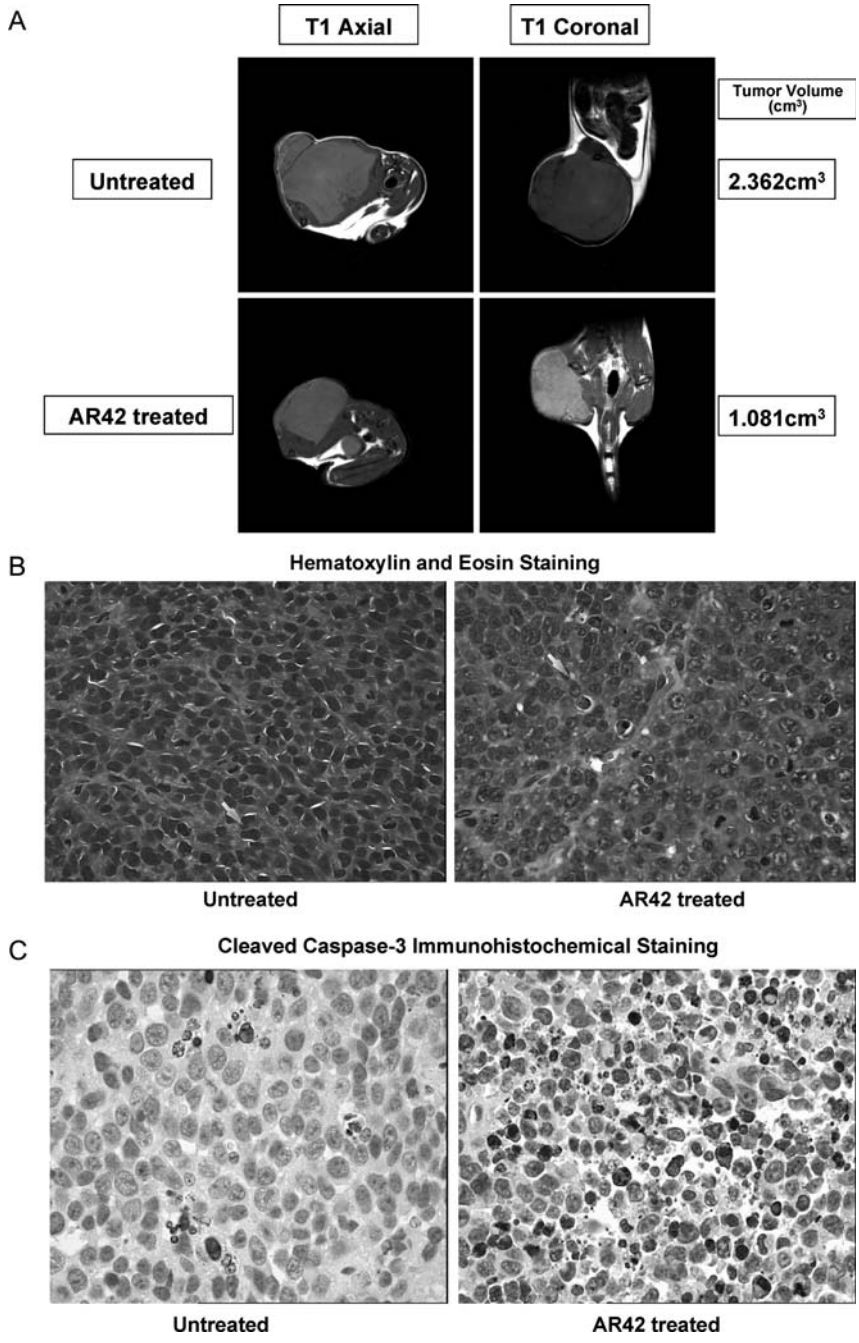

Fig. 6. AR42 treatment inhibits malignant schwannoma xenograft growth. HMS-97 cells (5×10^5 cells/mouse) were implanted in the left flank of SCID mice as previously described.[24] Xenograft-bearing mice were fed normal chow or AR42-containing chow formulated to deliver 25 mg/kg HDAC42 daily. The mice were weighed weekly and the amount of drug chow consumed was assessed weekly. Forty-five days following the injection, the mice were examined with a 9.4 T/cm MRI scanner, and noncontrasted T1-weighted axial and coronal images were obtained. Mice that had been fed AR42 had on average 42% smaller tumors compared with the control group (A). Tumor histopathology revealed an increase in apoptotic bodies on hematoxylin–eosin staining (B) that was confirmed by increased cleaved caspase-3 labeling (C). Apoptosis was also demonstrated with TUNEL staining, which showed strong staining in drug-treated tumors (D). Drug-treated tumors had decreased p-Akt(Ser473) labeling relative to control tumors (E).

p-Akt, and was not overtly toxic to mice. Interestingly, steady-state oral dosing of schwannoma xenograft-bearing mice for 45 days found robust evidence of apoptosis. Histologic analysis of hematoxylin-eosin sections from AR42-treated tumors revealed apoptotic bodies, and TUNEL staining and anticleaved caspase-3 antibody found increased staining throughout all treated specimens. These results demonstrate that the effect of AR42 may be cell type-dependent and may also depend on dose and duration of treatment. This

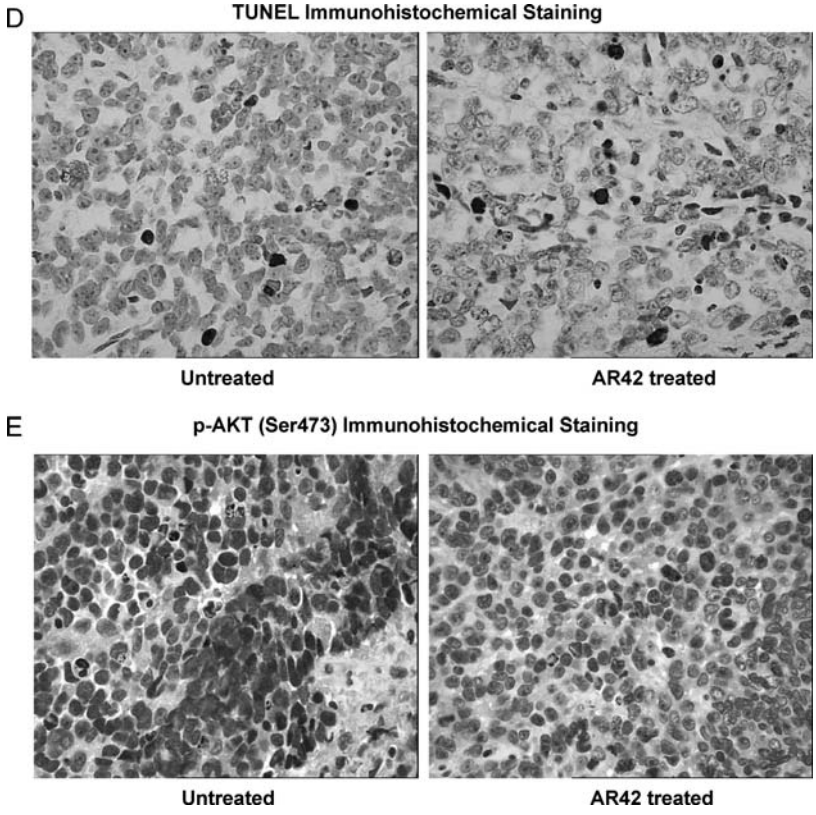

Fig. 6. (continued).

finding underscores the importance of validating in vitro drug mechanism studies using in vivo results. This is particularly relevant to the human condition in that oral dosing of AR42 likely results in steady drug levels for days or perhaps even weeks of treatment.

Our study findings are consistent with results from other investigators demonstrating that the in vivo efficacy of AR42 treatment correlates with suppression of Akt activation.[45,46,49,83] For example, AR42 suppressed PC-3 prostate cancer xenograft growth by reducing phospho-Akt as well as activating the intrinsic apoptotic pathway.[45] More than a dozen HDAC inhibitors are now being investigated in phase I/II clinical trials for solid and hematological tumors, with some showing efficacy and low pharmacotoxicity.[21,27,35,36,84] Due to its high potency against NF2-associated tumors through inhibitory effects on Akt, AR42 is a promising candidate for the treatment of VSs and meningiomas.

Conclusion

AR42 is a novel histone deacetylase inhibitor that potently reduces VS and meningioma proliferation. This growth suppression correlates with decreased Akt phosphorylation and G_2 cell cycle arrest and apoptosis induction. Consistently, in vivo treatment with AR42 inhibited the growth of schwannoma xenografts, induced apoptosis, and decreased activated Akt. Further validation of this novel small-molecule inhibitor as a potential treatment for VS and meningioma is warranted.

Acknowledgments

We sincerely thank Dr. Marco Giovannini and INSERM for P0Cre;$Nf2^{flox/flox2}$ mice; Drs. John McGregor, Daniel Prevedello, Brad Otto, and E. Antonio Chiocca for fresh meningioma specimens; Dr. Edward Dodson for VS specimens; the staff of the OSU Comparative Pathology and Mouse Phenotyping Shared Resource; the staff of the OSU Pathology Core Facility; the OSU Flow Cytometry Core Lab; Drs. Kimberly Powell and Anna Bratasz for small animal MRI imaging and volumetric tumor analysis; and Dr. Matthew Ringel for the use of laboratory space to perform some of the experiments. Tissue samples were provided by the Cooperative Human Tissue Network of The Ohio State University Comprehensive Cancer Center, which is funded by the National Cancer Institute. We also thank Beth Miles-Markley, M.S. for coordination of research subjects and critical review of this manuscript.

Conflict of interest statement. None declared.

Funding

National Institute of Deafness and Other Communication Disorders [ABJ – K08 DC009644-01A1; DBW – R01

DC005985 and 3R01DC005985-05S11], American Hearing Research Foundation [MLB – GRT00014844], Department of Defense [LSC – NF080021], Children's Tumor Foundation [ABJ – DDI 2007-05–2], and the Triological Society [ABJ – GRT00011359]

References

1. Rouleau GA, Merel P, Lutchman M, et al. Alteration in a new gene encoding a putative membrane-organizing protein causes neurofibromatosis type 2. *Nature*. 1993;363(6429):515–521.
2. Trofatter JA, MacCollin MM, Rutter JL, et al. A novel moesin-, ezrin-, radixin-like gene is a candidate for the neurofibromatosis 2 tumor suppressor. *Cell*. 1993;72(5):791–800.
3. Perry A, Louis DN, Scheithauer BW, et al. Meningiomas. In: Louis, D.N., Ohgaki, H., Wiestler, O.D., Cavenee, W.K., eds. WHO classification of tumours of the central nervous system. Lyon, France: IARC Press; 2007:164–172.
4. Son EI, Kim IM, Kim SP. Vestibular schwannoma with malignant transformation: a case report. *J Korean Med Sci*. 2001;16(6): 817–821.
5. Evans DG, Huson SM, Donnai D, et al. A genetic study of type 2 neurofibromatosis in the United Kingdom. II. Guidelines for genetic counselling. *J Med Genet*. 1992;29:847–852.
6. Gutmann DH, Giordano MJ, Fishback AS, et al. Loss of merlin expression in sporadic meningiomas, ependymomas and schwannomas. *Neurology*. 1997;49:267–270.
7. Wiemels J, Wrensch M, Claus EB. Epidemiology and etiology of meningioma. *J Neurooncol*. 2010;99(3):307–314. Epub 2010 Sep 7.
8. Welling DB, Packer MD, Chang LS. Molecular studies of vestibular schwannomas: a review. *Curr Opin Otolaryngol Head Neck Surg*. 2007;15(5):341–346.
9. Matthies C, Samii M. Management of 1000 vestibular schwannomas (acoustic neuromas): clinical presentation. *Neurosurgery*. 1997;40(1): 1–9; discussion 9–10.
10. Sauvaget E, Kici S, Kania R, et al. Sudden sensorineural hearing loss as a revealing symptom of vestibular schwannoma. *Acta Otolaryngol*. 2005;125(6):592–595.
11. Nageris BI, Popovtzer A. Acoustic neuroma in patients with completely resolved sudden hearing loss. *Ann Otol Rhinol Laryngol*. 2003;112(5): 395–397.
12. Kameda K, Shono T, Hashiguchi K, et al. Effect of tumor removal on tinnitus in patients with vestibular schwannoma. *J Neurosurg*. 2010; 112(1):152–157.
13. Evans DG. Neurofibromatosis type 2 (NF2): a clinical and molecular review. *Orphanet J Rare Dis*. 2009;4:16.
14. Levine EM, Becker Y, Boone CW, et al. Contact inhibition, macromolecular synthesis, and polyribosomes in cultured human diploid fibroblasts. *Proc Natl Acad Sci USA*. 1965;53:350–356.
15. Levine BB. Studies on delayed hypersensitivity. I. Inferences on the comparative binding affinities of antibodies mediating delayed and immediate hypersensitivity reactions in the guinea pig. *J Exp Med*. 1965;121:873–888.
16. Eagle H, Levine EM, Boone CW. Cellular growth, contact inhibition, and macromolecular synthesis. *Science*. 1965;148(3670):665.
17. Jacob A, Lee T, Neff BA, et al. Phosphatidylinositol 3-kinase/Akt pathway activation in human vestibular schwannoma. *Otol Neurotol*. 2008;29:58–68.
18. Mawrin C, Sasse T, Kirches E, et al. Different activation of mitogen-activated protein kinase and Akt signaling is associated with aggressive phenotype of human meningiomas. *Clin Cancer Res*. 2005;11(11): 4074–4082.
19. Lee TX, Packer MD, Huang J, et al. Growth inhibitory and anti-tumour activities of OSU-03012, a novel PDK-1 inhibitor, on vestibular schwannoma and malignant schwannoma cells. *Eur J Cancer*. 2009;45(9): 1709–1720.
20. Johnson MD, Okediji E, Woodard A, et al. Evidence for phosphatidylinositol 3-kinase Akt-p70S6K pathway activation and transduction of mitogenic signals by platelet derived growth factor in human meningioma cells. *J Neurosurg*. 2002;97:668–675.
21. Minucci S, Pelicci PG. Histone deacetylase inhibitors and the promise of epigenetic (and more) treatments for cancer. *Nat Rev Cancer*. 2006; 6:38–51.
22. Jung M. Inhibitors of histone deacetylase as new anticancer agents. *Curr Med Chem*. 2001;8:1505–1511.
23. Wade PA. Transcriptional control at regulatory checkpoints by histone deacetylases: molecular connections between cancer and chromatin. *Hum Mol Genet*. 2001;10:693–698.
24. Glaser KB, Staver MJ, Waring JF, et al. Gene expression profiling of multiple histone deacetylase (HDAC) inhibitors: defining a common gene set produced by HDAC inhibition in T24 and MDA carcinoma cell lines. *Mol Cancer Ther*. 2003;2:151–163.
25. Villar-Garea A, Esteller M. Histone deacetylase inhibitors: understanding a new wave of anticancer agents. *Int J Cancer*. 2004;112: 171–178.
26. Johnstone RW, Licht JD. Histone deacetylase inhibitors in cancer therapy: is transcription the primary target? *Cancer Cell*. 2003; 4:13–18.
27. Marks PA, Breslow R. Dimethyl sulfoxide to vorinostat: development of this histone deacetylase inhibitor as an anticancer drug. *Nat Biotechnol*. 2007;25:84–90.
28. Marks PA, Richon VM, Rifkind RA. Cell cycle regulatory proteins are targets for induced differentiation of transformed cells: molecular and clinical studies employing hybrid polar compounds. *Int J Hematol*. 1996;63:1–17.
29. Nimmanapalli R, Fuino L, Stobaugh C, et al. Cotreatment with the histone deacetylase inhibitor suberoylanilide hydroxamic acid (SAHA) enhances imatinib-induced apoptosis of Bcr-Abl-positive human acute leukemia cells. *Blood*. 2003;101:3236–3239.
30. Ungerstedt JS, Sowa Y, XuW S, et al. Role of thioredoxin in the response of normal and transformed cells to histone deacetylase inhibitors. *Proc Natl Acad Sci U S A*. 2005;102:673–678.
31. Xu W, Ngo L, Perez G, et al. Intrinsic apoptotic and thioredoxin pathways in human prostate cancer cell response to histone deacetylase inhibitor. *Proc Natl Acad Sci U S A*. 2006;103:15540–15545.
32. Marks PA, Dokmanovic M. Histone deacetylase inhibitors: discovery and development as anticancer agents. *Expert Opin Investig Drugs*. 2005;14:1497–1511.

33. Rosato RR, Maggio SC, Almenara JA, et al. The histone deacetylase inhibitor LAQ824 induces human leukemia cell death through a process involving XIAP down-regulation, oxidative injury, and the acid sphingomyelinase-dependent generation of ceramide. *Mol Pharmacol*. 2006;69:216–225.
34. Santini V, Gozzini A, Ferrari G. Histone deacetylase inhibitors: molecular and biological activity as a premise to clinical application. *Current Drug Metabolism*. 2007;8:383–394.
35. Bolden JE, Peart MJ, Johnstone RW. Anticancer activities of histone deacetylase inhibitors. *Nat Rev Drug Discov*. 2006;5:769–784.
36. Drummond DC, Noble CO, Kirpotin DB, et al. Clinical development of histone deacetylase inhibitors as anticancer agents. *Annu Rev Pharmacol Toxicol*. 2005;45:495–528.
37. Furchert SE, Lanvers-Kaminsky C, Juurgens H, et al. Inhibitors of histone deacetylases as potential therapeutic tools for high-risk embryonal tumors of the nervous system of childhood. *Int J Cancer*. 2007;120(8):1787–1794.
38. Shu Q, Antalffy B, Su JMF, et al. Valproic acid prolongs survival time of severe combined immunodeficiency mice bearing intracerebellar orthotopic medulloblastoma xenografts. *Clin Cancer Res*. 2006;12: 4687–4694.
39. Li XN, Shu Q, Su JM, et al. Valproic acid induces growth arrest apoptosis, and senescence in medulloblastoma by increasing histone hyperacetylation and regulating expression of p21Cip1, CDK4, and CMYC. *Mol Cancer Ther*. 2005;4(12):1912–1922.
40. Papi A, Ferreri AM, Rocchi P, et al. Epigenetic modifiers as anticancer drugs: effectiveness of valproic acid in neural crest-derived tumor cells. *Anticancer research*. 2010;30:535–540.
41. Knupfer MM, Hernaiz-Driever P, Poppenborg H, et al. Valproic acid inhibits proliferation and changes expression of CD44 and CD56 of malignant glioma cells in vitro. *Anticancer Res*. 1998;18: 3585–3589.
42. Sharma V, Koul N, Joseph C, et al. HDAC inhibitor, scriptaid induces glioma cell apoptosis through JNK activation and inhibits telomerase activity. *J Cell Mol Med*. 2010;14(8):2151–2161.
43. Chen CS, Weng SC, Tseng PH, et al. Histone acetylation- independent effect of histone deacetylase inhibitors on Akt through the reshuffling of protein phosphatase 1 complexes. *Bio Chem*. 2005;280(46): 38879–38887.
44. Bai LY, Omar HA, Chiu CF, et al. Antitumor effects of (S)- HDAC42, a phenylbutryate-derived histone deacetylase inhibitor, in multiple myeloma cells. *Cancer Chemother Pharmacol*. 2010;(Epub):1–8.
45. Sargeant AM, Rengel RC, Kulp SK, et al. OSU-HDAC42, a histone deacetylase inhibitor, blocks prostate tumor progression in the transgenic adenocarcinoma of the mouse prostate model. *Cancer Res*. 2008;68(10):3999–4009.
46. Lin TY, Fenger J, Murahari S, et al. AR-42, a novel HDAC inhibitor, exhibits biologic activity against malignant cell lines via down-regulation of constitutively activated Kit. *Blood*. 2010;115(21): 4217–4225.
47. Kulp SK, Chen CS, Wang DS, et al. Antitumor effects of a novel phenylbutyrate- based histone deacetylase inhibitor, (S)-HDAC-42, in prostate cancer. *Clin Cancer Res*. 2006;12(17):5199–5206.
48. Lu YS, Kashida Y, Kulp SK, et al. Efficacy of a novel histone deacetylase inhibitor in murine models of hepatocellular carcinoma. *Hepatology*. 2007;46(4): 1119–1130.
49. Yang YT, Balch C, Kulp SK, et al. A rationally designed histone deacetylase inhibitor with distinct antitumor activity against ovarian cancer. *Neoplasia*. 2009;11(6):552–563.
50. Giovannini M, Robanus-Maandag E, van der Valk M, et al. Conditional biallelic Nf2 mutation in the mouse promotes manifestations of human neurofibromatosis type 2. *Genes Dev*. 2000;14(13): 1617–1630.
51. Chang LS, Akhmametyeva EM, Wu Y, et al. Multiple transcription initiation sites, alternative splicing, and differential polyadenylation contribute to the complexity of human neurofibromatosis 2 transcripts. *Genomics*. 2002;79(1):63–76.
52. John MR, Wickert H, Zaar K, et al. A case of neuroendocrine oncogenic osteomalacia associated with a PHEX and fibroblast growth factor-23 expressing sinusidal malignant schwannoma. *Bone*. 2001;29:393–402.
53. Püttmann S, Senner V, Braune S, et al. Establishment of a benign meningioma cell line by hTERT-mediated immortalization. *Lab Invest*. 2005;85(9):1163–1171.
54. Klampfer L, Huang J, Shirasawa S, et al. Histone deacetylase inhibitors induce cell death selectively in cells that harbor activated kRasV12: the role of signal transducers and activators of transcription 1 and p21. *Cancer Res*. 2007;67:8477–8485.
55. Plotkin SR, Halpin C, McKenna MJ, et al. Erlotinib for progressive vestibular schwannoma in neurofibromatosis 2 patients. *Otol Neurotol*. 2010;31(7):1135–1143.
56. Evans DG, Kalamarides M, Hunter-Schaedle K, et al. Consensus recommendations to accelerate clinical trials for neurofibromatosis type 2. *Clin Cancer Res*. 2009;15(16):5032–5039.
57. Ammoun S, Cunliffe CH, Allen JC, et al. ErbB/HER receptor activation and preclinical efficacy of lapatinib in vestibular schwannoma. *Neuro Oncol*. 2010;12(8):834–843.
58. Plotkin SR, Stemmer-Rachamimov AO, Barker FG, et al. Hearing improvement after bevacizumab in patients with neurofibromatosis type 2. *N Engl J Med*. 2009;361(4):358–67.
59. Hilton DA, Ristic N, Hanemann CO. Activation of ERK, AKT and JNK signalling pathways in human schwannomas in situ. *Histopathology*. 2009;55(6):744–749.
60. Kaempchen K, Mielke K, Utermark T, et al. Upregulation of the Rac/JNK1 signaling pathway in primary human schwannoma cells. *Hum Mol Genet*. 2003;12(11):1211–1221.
61. Shaw RJ, Paez JG, Curto M, et al. The Nf2 tumor suppressor, merlin, functions in Rac-dependent signaling. *Dev Cell*. 2001;1(1):63–72.
62. Scoles DR. The merlin interacting proteins reveal multiple targets for NF2 therapy. *Biochim Biophys Acta,*. 2008;1785(1):32–54.
63. Curto M, McClatchey AI. Nf2/Merlin: a coordinator of receptor signalling and intercellular contact. *Br J Cancer*. 2008;98(2):256–262.
64. Maitra S, Kulikauskas RM, Gavilan H, et al. The tumor suppressors Merlin and Expanded function cooperatively to modulate receptor endocytosis and signaling. *Curr Biol*. 2006;16(7):702–709.
65. Curto M, Cole BK, Lallemand D, et al. Contact-dependent inhibition of EGFR signaling by Nf2/Merlin. *J Cell Biol*. 2007;177(5):893–903.
66. James MF, Beauchamp RL, Manchanda N et al. A NHERF binding site links the betaPDGFR to the cytoskeleton and regulates cell spreading and migration. *J Cell Sci*. 2004;117(Pt 14):2951–2961.
67. McClatchey AI, Fehon RG. Merlin and the ERM proteins–regulators of receptor distribution and signaling at the cell cortex. *Trends Cell Biol*. 2009;19(5):198–206.
68. Andrae J, Gallini R, Betsholtz C. Role of platelet-derived growth factors in physiology and medicine. *Genes Dev*. 2008;22(10): 1276–1312.
69. Li W, Nishimura R, Kashishian A, et al. A new function for a phosphotyrosine phosphatase: linking GRB2-Sos to a receptor tyrosine kinase. *Mol Cell Biol*. 1994;14(1):509–517.

70. Roux PP, Blenis J. ERK and p38 MAPK-activated protein kinases: a family of protein kinases with diverse biological functions. *Microbiol Mol Biol Rev*. 2004;68(2):320–344.
71. Treisman R. Regulation of transcription by MAP kinase cascades. *Curr Opin Cell Biol*. 1996;8(2):205–215.
72. Altomare DA, Testa JR. Perturbations of the AKT signaling pathway in human cancer. *Oncogene*. 2005;24(50):7455–7464.
73. Coffer PJ, Jin J, Woodgett JR. Protein kinase B (c-Akt): a multifunctional mediator of phosphatidylinositol 3-kinase activation. *Biochem J*. 1998;335(Pt 1):1–13.
74. Johnson MD, O'Connell M, Vito F, et al.. Increased STAT-3 and synchronous activation of Raf-1-MEK-1-MAPK, and phosphatidylinositol 3- Kinase-Akt-mTOR pathways in atypical and anaplastic meningiomas. *J Neurooncol*. 2009;92(2):129–136.
75. Johnson M, Toms S. Mitogenic signal transduction pathways in meningiomas: novel targets for meningioma chemotherapy? *J Neuropathol Exp Neurol*. 2005;64(12):1029–1036.
76. Jin HO, Park IC, An S, et al. Up-regulation of Bak and Bim via JNK downstream pathway in the response to nitric oxide in human glioblastoma cells. *J Cell Physiol*. 2006;206:477–786.
77. Xia S, Li Y, Rosen EM, et al. Ribotoxic stress sensitizes glioblastoma cells to death receptor induced apoptosis: requirements for c-Jun NH2-terminal kinase and Bim. *Mol Cancer Res*. 2007;5: 783–792.
78. Dai Y, Rahmani M, Dent P, et al. Blockade of histone deacetylase inhibitor induced RelA/p65 acetylation and NFkappaB activation potentiates apoptosis in leukemia cells through a process mediated by oxidative damage, XIAP downregulation, and c-Jun N-terminal kinase 1 activation. *Mol Cell Biol*. 2005;25: 5429–5444.
79. Minden A, Lin A, McMahon M, et al. Differential activation of ERK and JNK mitogen-activated protein kinases by Raf-1 and MEKK. *Science*. 1994;266:1719–1723.
80. Cress WD, Seto E. Histone deacetylases, transcriptional control, and cancer. *J Cell Physiol*. 2000;184:1–16.
81. Marks P, Rifkind RA, Richon VM, Breslow R, Miller T, Kelly WK. Histone deacetylases and cancer: causes and therapies. *Nat Rev Cancer*. 2001;1:194–202.
82. Lee EJ, Lee BB, Kim SJ, Park YD, Park J, Kim DH. Histone deacetylase inhibitor scriptaid induces cell cycle arrest and epigenetic change in colon cancer cells. *International Journal of Oncology*. 2008;33:767–776.
83. Lucas DM, Alinari L, West DA, et al. The novel deacetylase inhibitor AR-42 demonstrates pre-clinical activity in B-cell malignancies in vitro and in vivo. *PLoS One*. 2010;5(6):e10941.
84. Johnson MD, O'Connell M, Pilcher W. Lopinavir inhibits meningioma cell proliferation by Akt independent mechanism. *J Neurooncol*. 2011;101(3):441–448.